Supporting Information for

Thermally Activated Delayed Fluorescence and Mechanochromism in Napthalimide-Azatriangulenes

By Seja A. Elgadi[†], Ying Cai[†], and Zachary M. Hudson*

Department of Chemistry, The University of British Columbia, 2036 Main Mall, Vancouver, British Columbia, Canada, V6T 1Z1.

Tel: +1-604-822-3266; Fax: +1-604-822-2847; e-mail: zhudson@chem.ubc.ca.

[†] *These authors contributed equally to this work.*

Table of Contents

Experimental Details 2
Synthetic Schemes 3
Synthetic Procedures 4
^{1}H and ^{13}C{^{1}H} NMR Spectra 6
X-ray Crystallography 14
Photophysical Characterization 11
Thermal and Electrochemical Characterization 17
Density Functional Theory 18
References 22

Experimental Details

General Considerations. All reactions and manipulations were carried out under a nitrogen atmosphere using standard Schlenk or glove box techniques unless otherwise stated. Dry and degassed toluene and tetrahydrofuran were obtained from Caledon Laboratories, dried using an Innovative Technologies Inc. solvent purification system. 1,4-dioxane was dried over 4 Å molecular sieves. All reagents were obtained from Sigma-Aldrich, TCI America, Pressure Chemical, or Oakwood Chemical, and used as received unless otherwise stated. SMAT-Br, HMAT-Br, OMAT, and NAI-Br were prepared according to literature procedures.[1–4] The ^{1}H and $^{13}C\{^{1}H\}$ nuclear magnetic resonance (NMR) spectra were measured on a Bruker AV III HD 400 MHz spectrometer with chloroform-*d* ($CDCl_3$), dichloromethane-d_2 (CD_2Cl_2), or dimethylsulfoxide-d_6 (DMSO-d_6) as the solvent. Mass spectra were recorded on a Bruker HCTultra PTM Discovery System using electrospray ionization (ESI).

General Photophysical Characterization. Absorbance measurements were made on a Cary 60 spectrometer and fluorescence measurements were made on an Edinburgh Instruments FS5 spectrofluorometer or Edinburgh Instruments FLS1000 spectrofluorometer. Concentrations of 0.01 mg mL^{-1} were used unless otherwise stated. Absolute photoluminescence quantum yields were determined using an Edinburgh Instruments SC–30 Integrating Sphere Module, with optical densities less than 0.1. Lifetimes were obtained using an Edinburgh Instruments EPLED source (λ_{exc} = 380 nm) coupled with time-correlated single-photon counting (TCSPC), or a Xe μF lamp coupled with multichannel scaling (MCS). All samples were excited at the maximum of the lowest energy absorption band and lifetimes were measured at the fluorescence maximum unless otherwise specified.

Electrochemical Methods. Cyclic voltammograms were recorded using a BASi Epsilon Eclipse potentiostat at room temperature using a standard three-electrode configuration (working electrode: 3 mm diameter glassy carbon; reference electrode: RE-5B Ag/AgCl electrode in saturated aqueous KCl (BASi Inc.), referenced externally to ferrocene/ferrocenium, counter electrode: Pt wire) in 0.2 M tetrabutylammonium hexafluorophosphate in *o*-difluorobenzene. Experiments were run at a scan rate of 50 mV s^{-1} in degassed electrolyte solution with 1.0 μmol mL^{-1} of analyte.

Density Functional Theory. Quantum mechanical calculations were performed using the Gaussian 16 Rev. B.01 computational package using default settings unless otherwise stated. All geometries were optimized to a minimum, and frequency calculations were performed at the same level of theory to verify the absence of imaginary frequencies. Initial geometry optimizations were conducted at the B3LYP/6-31+g(d) level. Vertical excitation (absorption) energies of the lowest singlet and triplet excited states were calculated by the Tamm−Dancoff approximation (TDA) scheme of time-dependent DFT (TDA-TDDFT) at the B3LYP/6-31+g(d) level in toluene using the polarizable continuum model (PCM). The GD3BJ empirical dispersion correction was used in all calculations.

Synthetic Schemes

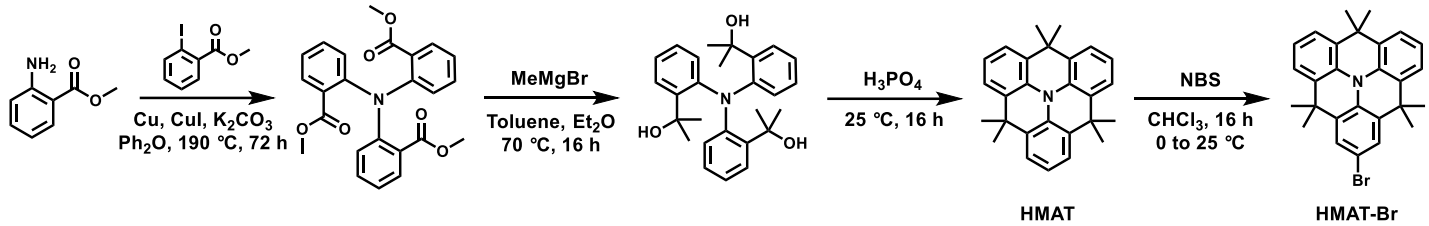

Scheme S1. Synthesis of **HMAT-Br**.

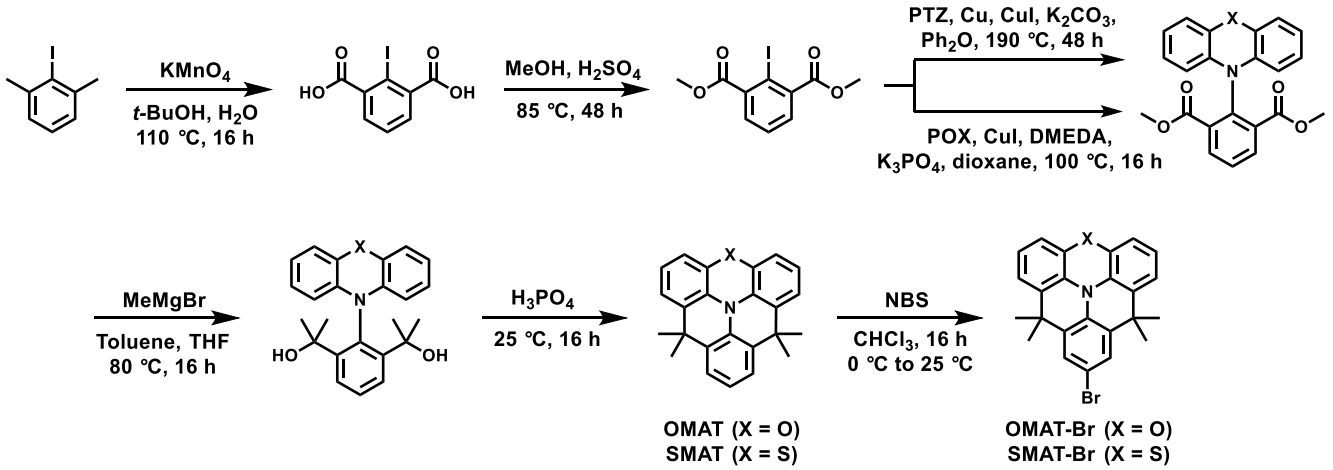

Scheme S2. Synthesis of planar donors **SMAT-Br** and **OMAT-Br**. PTZ = 10*H*-phenothiazine, POX = 10*H*-phenoxazine.

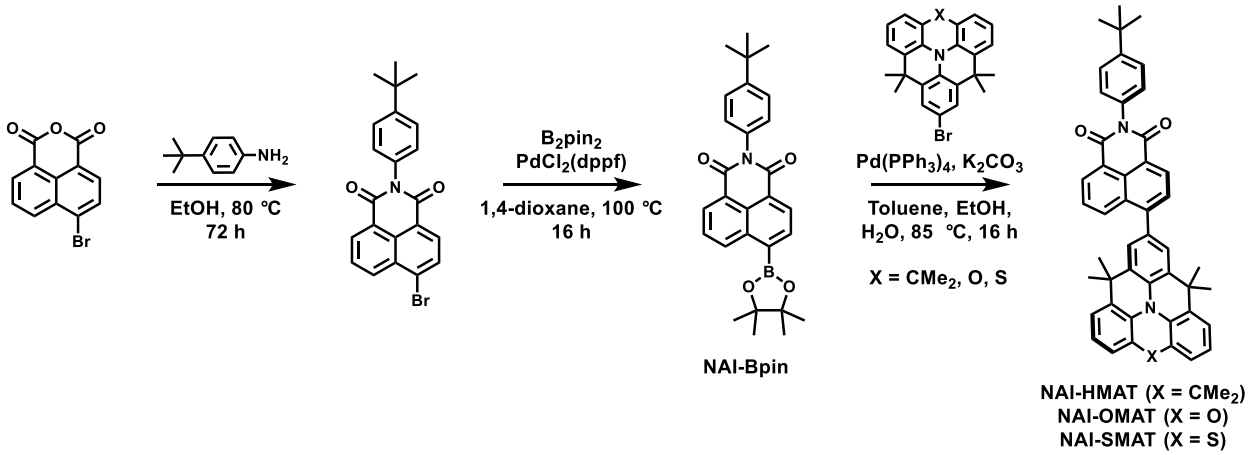

Scheme S3. Synthesis of **NAI-HMAT**, **NAI-OMAT**, and **NAI-SMAT**.

Synthetic Procedures

OMAT-Br

A 50 mL round bottom flask was charged with **OMAT** (266 mg, 0.784 mmol) which was dissolved in 15 mL $CHCl_3$ and cooled to 0 °C in an ice bath. The flask was covered with aluminum foil and *N*-bromosuccinimide (140 mg, 0.786 mmol, 1 equiv.) was dissolved in 8 mL $CHCl_3$ and added to the reaction dropwise with a Pasteur pipette. Subsequently, the ice bath was removed, and the reaction was allowed to warm to room temperature and proceed for 16 hours. After completion, the reaction was quenched with saturated aqueous $Na_2S_2O_3$ (50 mL) and the mixture was extracted with dichloromethane (3 × 50 mL). The combined organics were washed with deionized water (80 mL) and saturated brine (50 mL) then dried over anhydrous $MgSO_4$ and evaporated under reduced pressure. The resulting brown residue was purified by silica column chromatography using a gradient of hexanes to 2% toluene, 98% hexanes. Yield: white solid, 225 mg, 69%. ^{1}H NMR (400 MHz, DMSO-d_6) δ 7.53 (s, 2H), 7.11 (d, J = 7.0 Hz, 2H), 6.90 (t, J = 7.9 Hz, 2H), 6.67 (d, J = 7.8 Hz, 2H), 1.57 ppm (s, 12H). ^{13}C NMR (101 MHz, DMSO-d_6) δ 140.9, 130.6, 129.6, 127.9, 127.4, 124.0, 122.3, 121.3, 114.6, 113.5, 35.2, 33.2 ppm. HRMS (ESI) m/z: [M]+• calcd for $[C_{24}H_{20}BrNO]^{+\bullet}$, 417.0728; found, 417.0730; difference: 0.44 ppm.

NAI-Bpin

A dry 100 mL Schlenk flask was charged with **NAI-Br** (1.000 g, 2.45 mmol), B_2Pin_2 (933 mg, 3.67 mmol, 1.5 equiv.), KOAc (721 mg, 7.35 mmol, 3 equiv.), and $PdCl_2$(dppf) (90 mg, 0.12 mmol, 0.05 equiv.) in an N_2 atmosphere. Dry dioxane (30 mL) was transferred into the reaction flask by cannula and the mixture was degassed by sparging with N_2 gas while stirring for 10 mins. The reaction was heated to 90 °C for 16 hours before being taken off heat and diluted with CH_2Cl_2 (150 mL). The dark brown solution was washed with water (3 × 100 mL) and saturated brine (1 × 100 mL). The organic layer was dried over anhydrous $MgSO_4$ and evaporated under reduced pressure to yield a dark brown solid. The crude product was purified by silica column chromatography using a gradient of 40% CH_2Cl_2, 60% hexanes to CH_2Cl_2. Yield: Pale yellow solid, 423 mg, 38%.^{1}H NMR (400 MHz, Methylene Chloride-d_2) δ 9.20 (d, J = 8.4 Hz, 1H), 8.64 – 8.52 (m, 2H), 8.32 (d, J = 7.2 Hz, 1H), 7.83 (t, J = 7.8 Hz, 1H), 7.59 (d, J = 8.3 Hz, 2H), 7.23 (d, J = 8.3 Hz, 2H), 1.46 (s, 12H), 1.42 ppm (s, 9H). ^{13}C NMR (75 MHz, Chloroform-d) δ 164.74, 164.70, 151.5, 136.0, 135.6, 135.4, 132.7, 131.4, 130.3, 128.4, 128.1, 127.3, 126.6, 125.1, 122.9, 84.8, 34.9, 31.5, 25.1 ppm (quaternary carbon next to B was not visible). HRMS (ESI) m/z: [M]+• calcd for $[C_{28}H_{30}BNO_4]^{+\bullet}$, 454.2304; found, 454.2311; difference: 1.39 ppm.

NAI-HMAT

A dry 100 mL Schlenk flask was charged with **HMAT-Br** (124 mg, 0.279 mmol), **NAI-Bpin** (140 mg, 0.307 mmol, 1.1 equiv.), Na_2CO_3 (150 mg, 1.42 mmol, 5 equiv.), and $Pd(PPh_3)_4$ (10 mg, 0.0087 mmol, 0.03 equiv.) under a N_2 atmosphere. In a separate 50 mL round bottom flask, toluene (9 mL), ethanol (3 mL), and deionized water (1 mL) were sparged with N_2 gas for 30 minutes with vigorous stirring before being transferred into the reaction flask by cannula. The reaction was heated to 75 °C in an oil bath for 16 hours. After completion by TLC, the reaction was diluted with deionized water (50 mL) and the reaction mixture was extracted with dichloromethane (3 × 70 mL). The combined organics were washed with deionized water (70 mL) and saturated brine (70 mL) before being dried over anhydrous $MgSO_4$ and evaporated under reduced pressure. The resulting solid was purified by silica column chromatography using toluene. Yield: orange solid,

142 mg, 73%. ^{1}H NMR (400 MHz, DMSO-d_6) δ 8.62 – 8.52 (m, 2H), 8.43 (dd, J = 8.5, 1.1 Hz, 1H), 8.00 (d, J = 7.6 Hz, 1H), 7.90 (dd, J = 8.6, 7.2 Hz, 1H), 7.66 (s, 2H), 7.56 (d, J = 8.5 Hz, 2H), 7.50 (d, J = 7.7 Hz, 4H), 7.32 (d, J = 8.5 Hz, 2H), 7.20 (t, J = 7.7 Hz, 2H), 1.66 (s, 12H), 1.62 (s, 6H), 1.38 ppm (s, 9H). ^{13}C NMR (101 MHz, Methylene Chloride-d_2) δ 165.1, 164.9, 152.2, 148.1, 133.9, 133.7, 133.5, 133.1, 132.2, 131.8, 131.6, 131.0, 130.8, 130.4, 129.9, 128.9, 128.1, 127.4, 126.8, 125.8, 124.5, 124.2, 123.9, 123.8, 122.1, 36.2, 36.1, 35.3, 33.7, 33.4, 31.7 ppm. HRMS (ESI) m/z: [M]+• calcd for $[C_{49}H_{44}N_2O_2]^{+\bullet}$, 692.3403; found, 692.3405; difference: 0.33 ppm.

NAI-OMAT

A dry 100 mL Schlenk flask was charged with **NAI-Bpin** (60 mg, 0.132 mmol), **OMAT-Br** (61 mg, 0.145 mmol, 1.1 equiv.), Na_2CO_3 (70 mg, 0.66 mmol, 5 equiv.), and $Pd(PPh_3)_4$ (5 mg, 0.0043 mmol, 0.03 equiv.) under a N_2 atmosphere. In a separate 50 mL round bottom flask, toluene (9 mL), ethanol (3 mL), and deionized water (1 mL) were sparged with N_2 gas for 30 minutes with vigorous stirring before being transferred into the reaction flask by cannula. The reaction was heated to 75 °C in an oil bath for 16 hours. After completion by TLC, the reaction was diluted with deionized water (50 mL) and the reaction mixture was extracted with dichloromethane (3 × 70 mL). The combined organics were washed with deionized water (70 mL) and saturated brine (70 mL) before being dried over anhydrous $MgSO_4$ and evaporated under reduced pressure. The resulting solid was purified by silica column chromatography using 80% toluene, 20% $CHCl_3$. Yield: orange solid, 53 mg, 60 %. ^{1}H NMR (400 MHz, DMSO-d_6) δ 8.56 (d, J = 7.5 Hz, 2H), 8.39 (d, J = 8.3 Hz, 1H), 7.99 – 7.88 (m, 2H), 7.63 (s, 2H), 7.56 (d, J = 8.5 Hz, 2H), 7.32 (d, J = 8.4 Hz, 2H), 7.18 (d, J = 8.0 Hz, 2H), 6.95 (t, J = 7.9 Hz, 2H), 6.73 (d, J = 6.7 Hz, 2H), 1.68 (s, 12H), 1.38 ppm (s, 9H). ^{13}C NMR (101 MHz, Methylene Chloride-d_2) δ 165.1, 164.9, 152.2, 147.9, 142.6, 133.9, 133.5, 133.2, 131.8, 131.6, 130.9, 130.8, 130.5, 129.9, 129.4, 128.9, 128.1, 127.4, 126.9, 126.8, 124.4, 123.9, 123.8, 122.1, 121.4, 114.1, 36.1, 35.3, 33.9, 31.7 ppm. HRMS (ESI) m/z: [M]+• calcd for $[C_{46}H_{38}N_2O_3]^{+\bullet}$, 666.2882; found, 666.2882; difference: -0.11 ppm.

NAI-SMAT

A dry 100 mL Schlenk flask was charged with **NAI-Bpin** (200 mg, 0.439 mmol), **SMAT-Br** (210 mg, 0.483 mmol, 1.1 equiv.), Na_2CO_3 (233 mg, 2.20 mmol, 5 equiv.), and $Pd(PPh_3)_4$ (15 mg, 0.013 mmol, 0.03 equiv.) under a N_2 atmosphere. In a separate 50 mL round bottom flask, toluene (9 mL), ethanol (3 mL), and deionized water (1 mL) were sparged with N_2 gas for 30 minutes with vigorous stirring before being transferred into the reaction flask by cannula. The reaction was heated to 75 °C in an oil bath for 16 hours. After completion by TLC, the reaction was diluted with deionized water (50 mL) and the reaction mixture was extracted with dichloromethane (3 × 70 mL). The combined organics were washed with deionized water (70 mL) and saturated brine (70 mL) before being dried over anhydrous $MgSO_4$ and evaporated under reduced pressure. The resulting solid was purified by silica column chromatography using toluene. Yield: orange solid, 227 mg, 76 %. ^{1}H NMR (400 MHz, DMSO-d_6) δ 8.64 – 8.48 (m, 2H), 8.39 (d, J = 9.1 Hz, 1H), 7.99 (d, J = 7.6 Hz, 1H), 7.91 (t, J = 7.4 Hz, 1H), 7.64 (s, 2H), 7.56 (d, J = 8.5 Hz, 2H), 7.43 – 7.27 (m, 4H), 7.05 (t, J = 7.6 Hz, 2H), 6.92 (dd, J = 7.5, 1.5 Hz, 2H), 1.63 (s, 12H), 1.38 ppm (s, 9H). ^{13}C NMR (101 MHz, Methylene Chloride-d_2) δ 165.1, 164.9, 152.2, 147.7, 134.3, 133.9, 133.5, 132.8, 131.8, 131.6, 131.5, 130.9, 130.6, 129.8, 128.8, 128.2, 127.4, 126.8, 125.7, 125.2, 124.9, 123.8, 122.2, 117.1, 36.1, 35.3, 33.1, 31.7 ppm. HRMS (ESI) m/z: [M]+• calcd for $[C_{46}H_{38}N_2O_2S]^{+\bullet}$, 682.2654; found, 682.2654; difference: -0.73 ppm.

^{1}H and ^{13}C{^{1}H} NMR Spectra

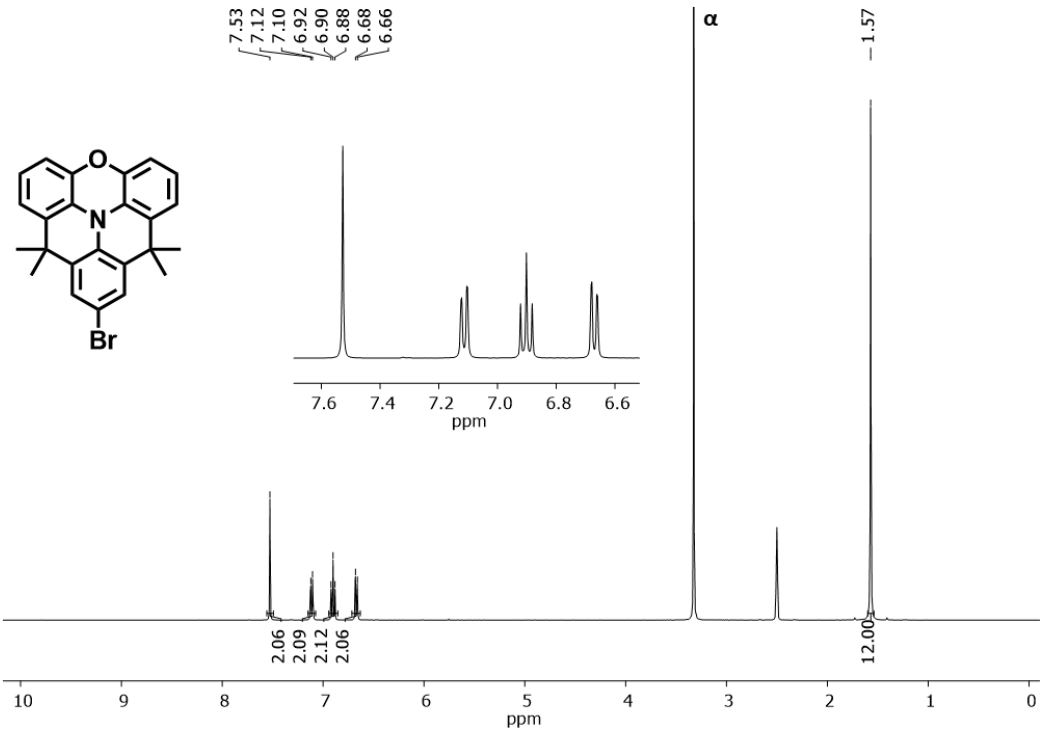

Figure S1. ^{1}H NMR (400 MHz, 25 °C) of **OMAT-Br** in DMSO-d_6 (**α**: H_2O).

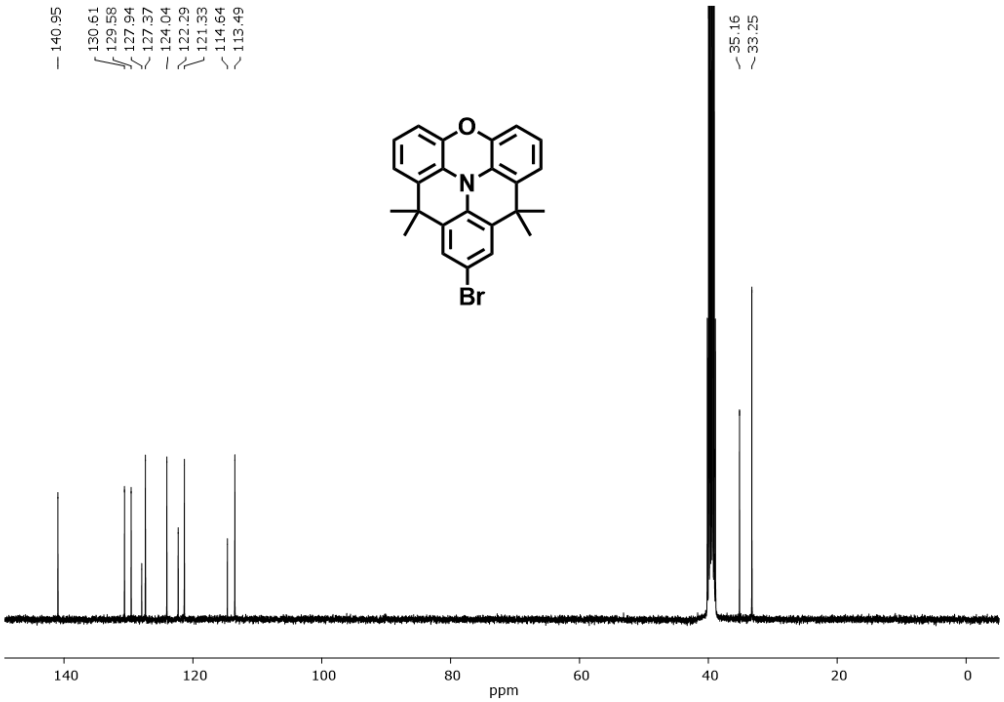

Figure S2. ^{13}C{^{1}H} NMR (101 MHz, 25 °C) of **OMAT-Br** in DMSO-d_6.

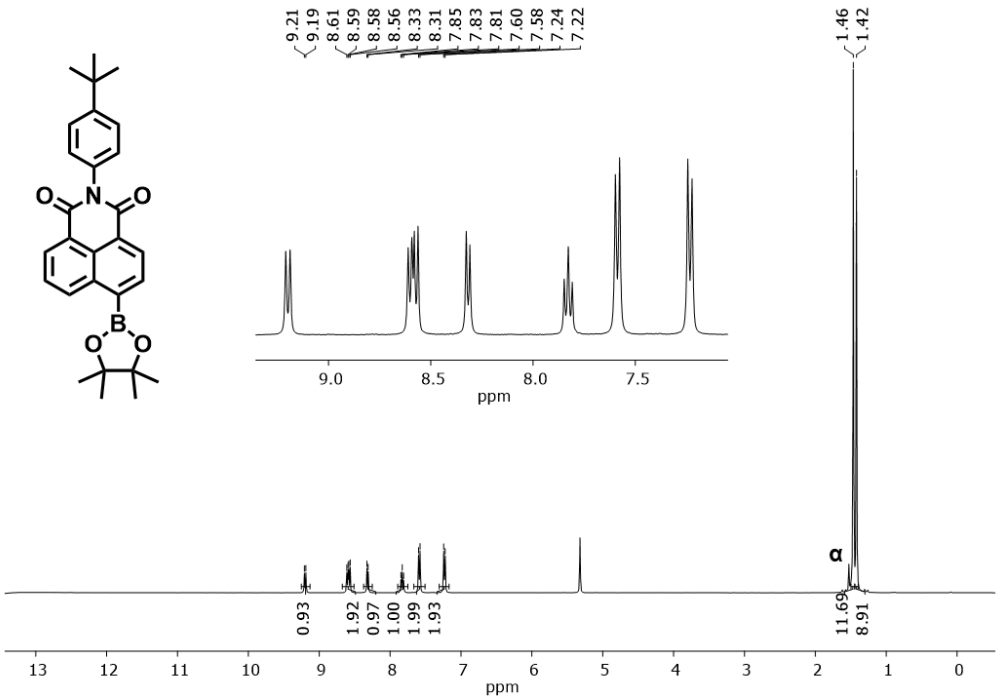

Figure S3. ^{1}H NMR (400 MHz, 25 °C) of **NAI-Bpin** in CD_2Cl_2 (***α***: H_2O).

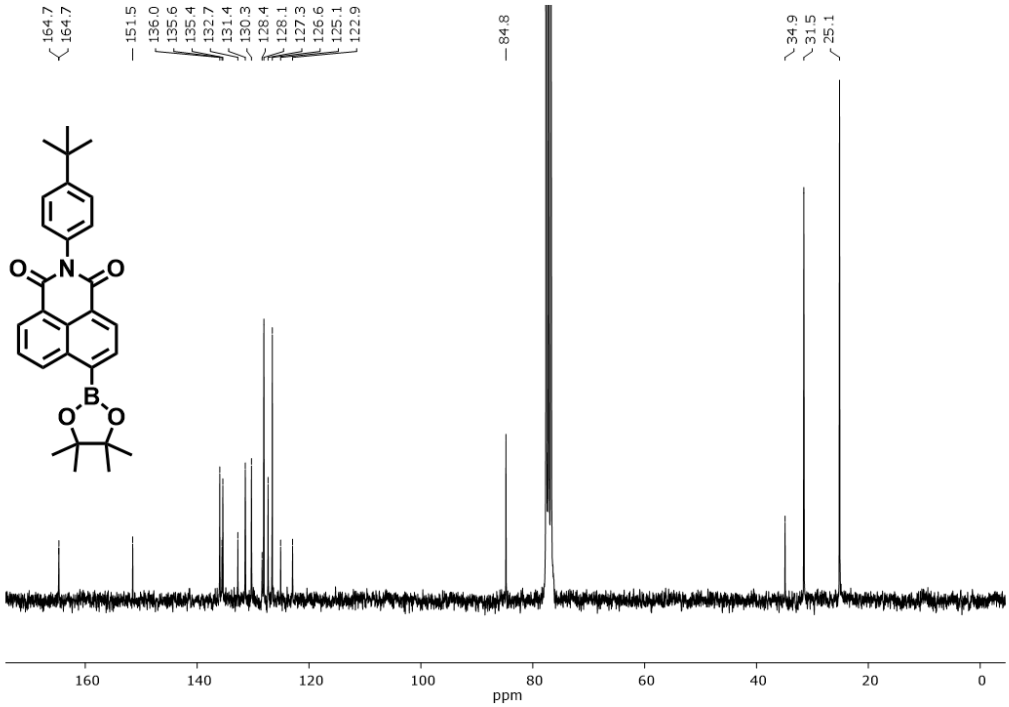

Figure S4. $^{13}C\{^{1}H\}$ NMR (75 MHz, 25 °C) of **NAI-Bpin** in $CDCl_3$.

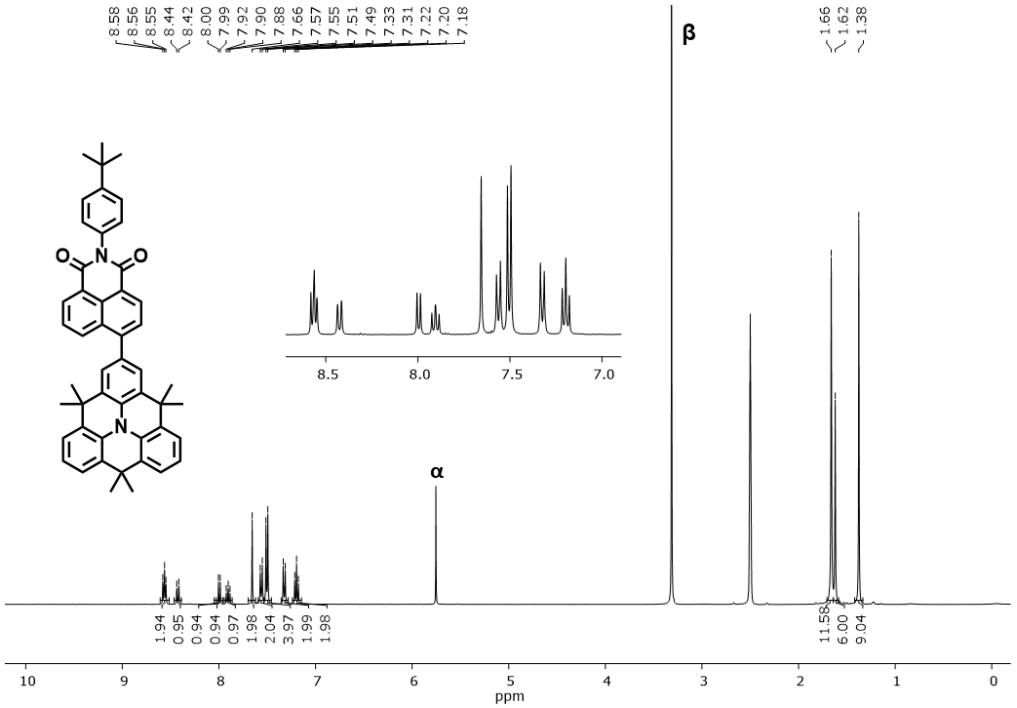

Figure S5. ^{1}H NMR (400 MHz, 25 °C) of **NAI-HMAT** in DMSO-d_6 (***α***: CH_2Cl_2, **β**: H_2O).

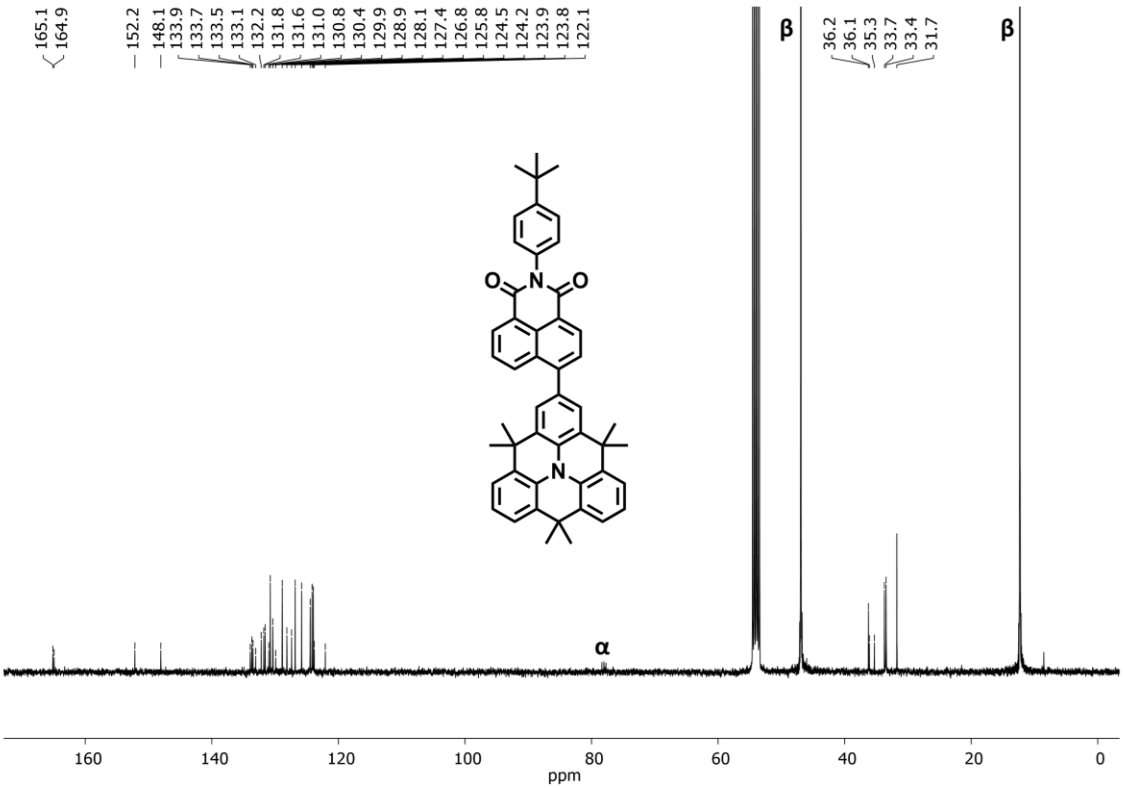

Figure S6. ^{13}C{^{1}H} NMR (101 MHz, 25 °C) of **NAI-HMAT** in CD_2Cl_2 with a drop of NEt_3 (***α***: $CHCl_3$, **β**: NEt_3).

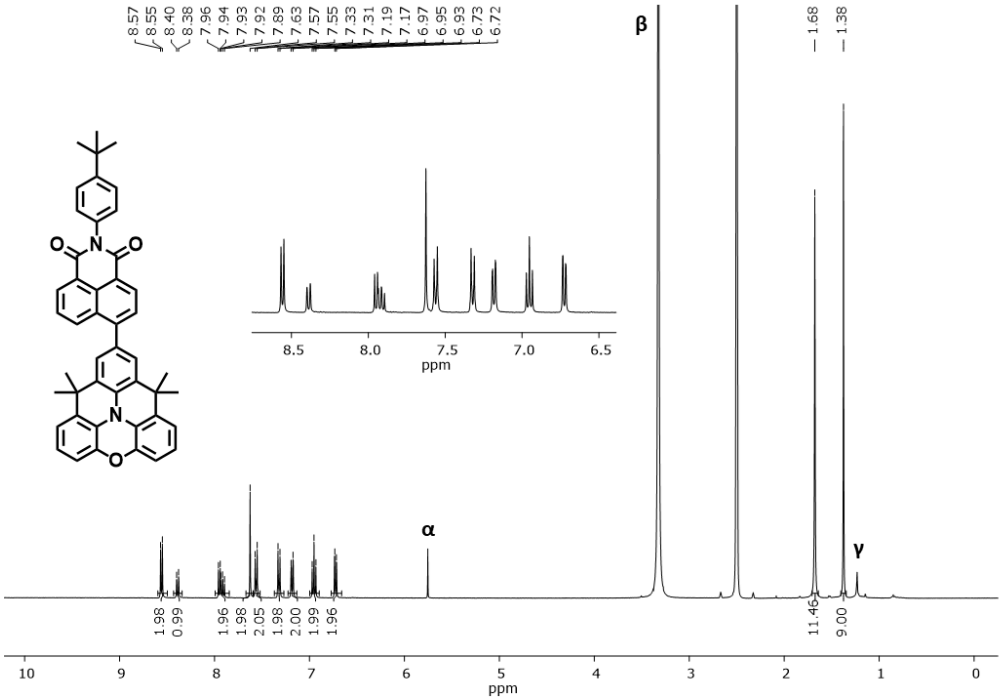

Figure S7. ^{1}H NMR (400 MHz, 25 °C) of **NAI-OMAT** in DMSO-d_6 (**α**: CH_2Cl_2, **β**: H_2O, **γ**: hexanes).

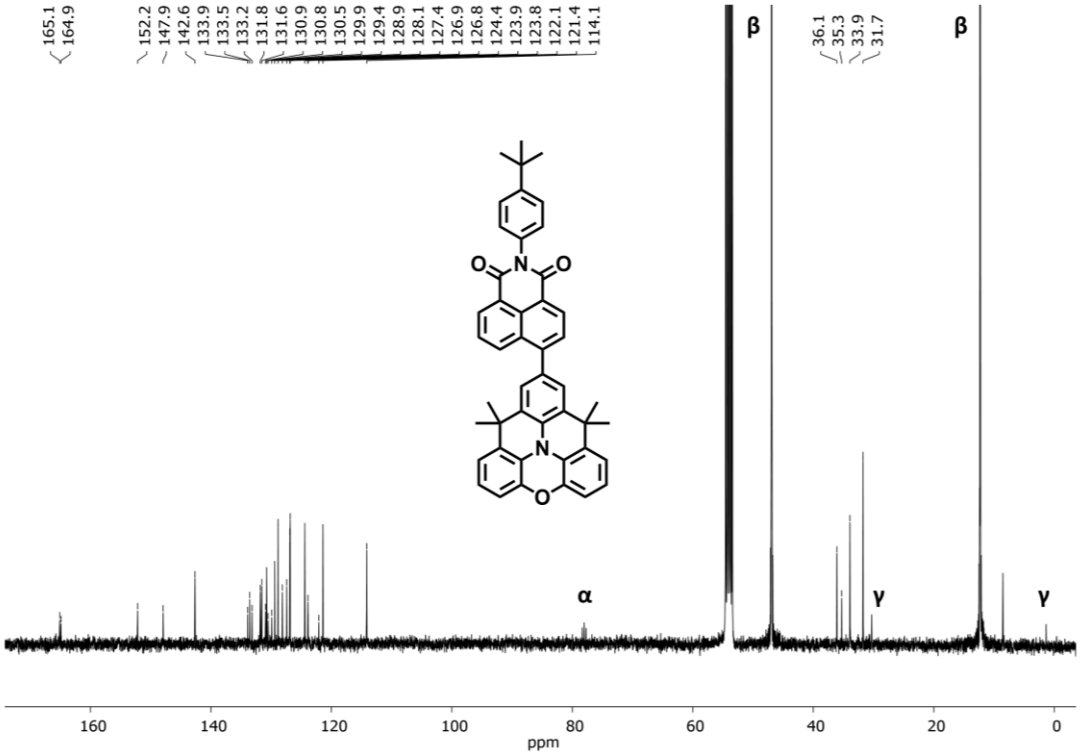

Figure S8. ^{13}C{^{1}H} NMR (101 MHz, 25 °C) of **NAI-OMAT** in CD_2Cl_2 with a drop of NEt_3 (**α**: $CHCl_3$, **β**: NEt_3, **γ**: grease).

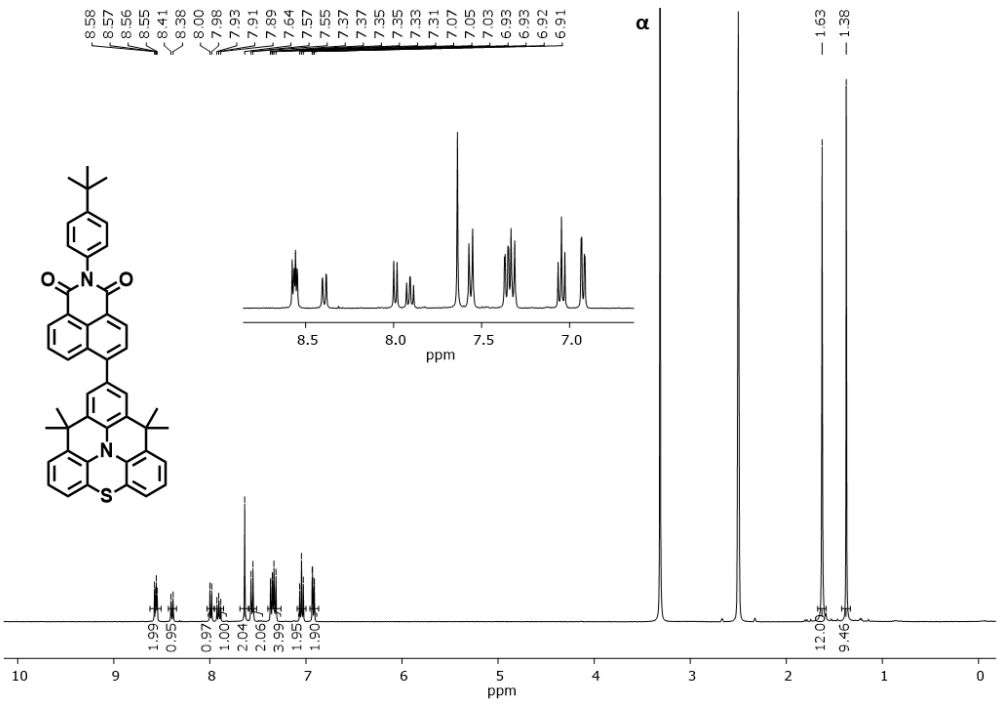

Figure S9. ^{1}H NMR (400 MHz, 25 °C) of **NAI-SMAT** in DMSO-d_6 (**α**: H_2O).

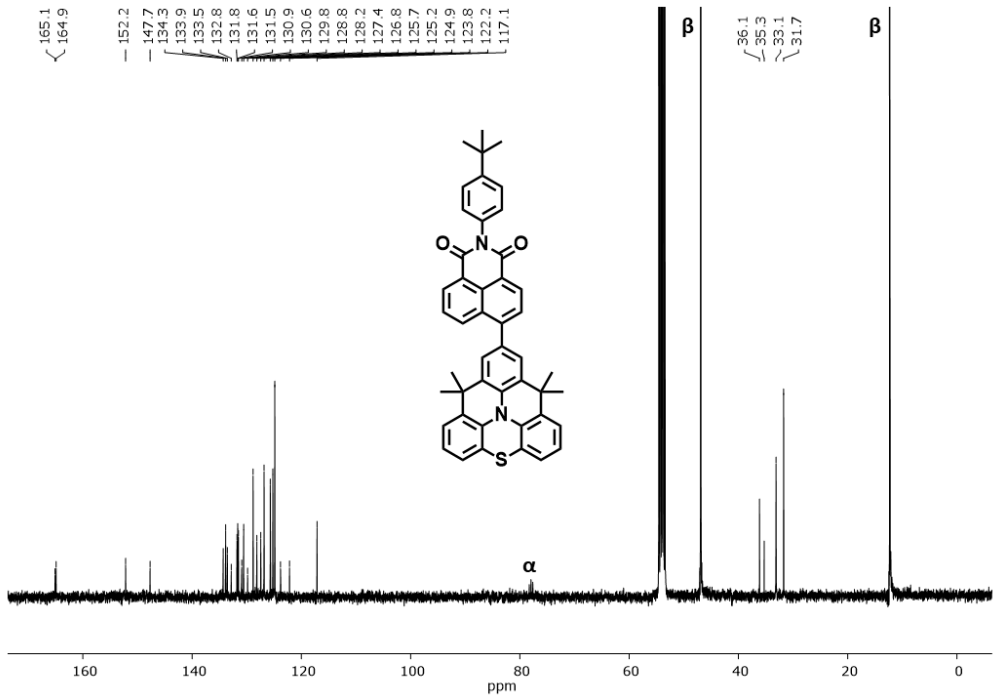

Figure S10. ^{13}C{^{1}H} NMR (101 MHz, 25 °C) of **NAI-SMAT** in CD_2Cl_2 with a drop of NEt_3 (**α**: $CHCl_3$, **β**: NEt_3).

Photophysical Characterization

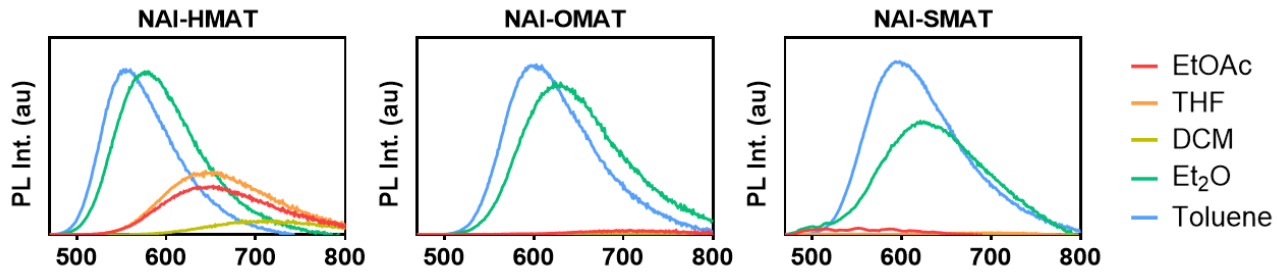

Figure S11. Emission spectra in solvents of varying polarity. Measured at concentrations of 1.0×10^{-2} mg mL^{-1}.

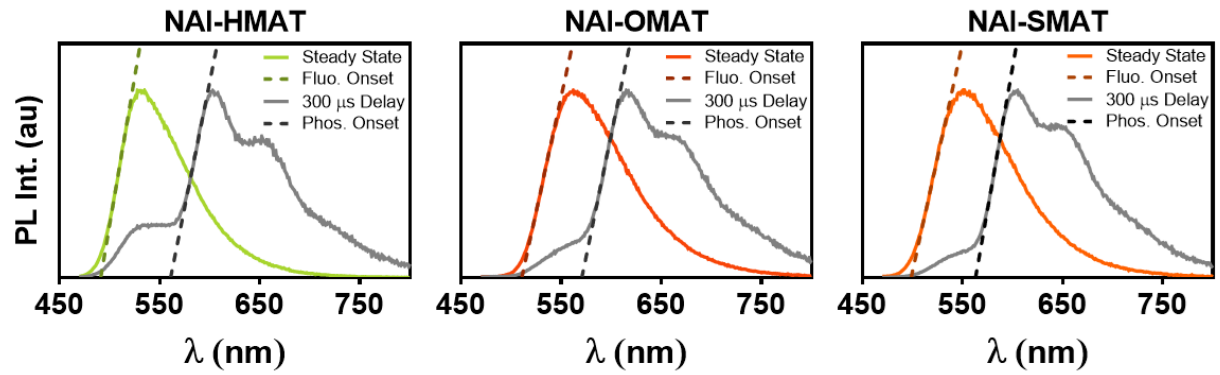

Figure S12. Steady-state fluorescence (coloured) and time-gated phosphorescence (gray) spectra measured at 77K, with corresponding linear onset fits. Samples were measured at 1.0×10^{-2} mg mL^{-1} in 2-methyltetrahydrofuran.

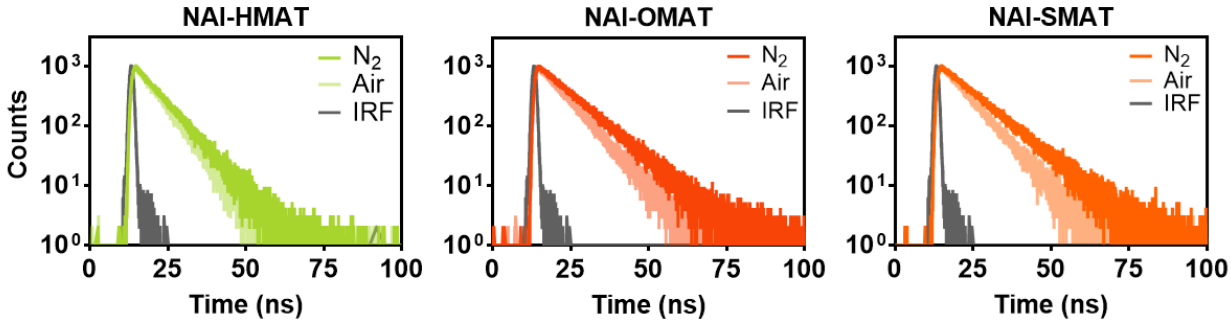

Figure S13. Photoluminescence decays of each emitter in toluene (1.0×10^{-2} mg mL^{-1}) under N_2 and aerated conditions.

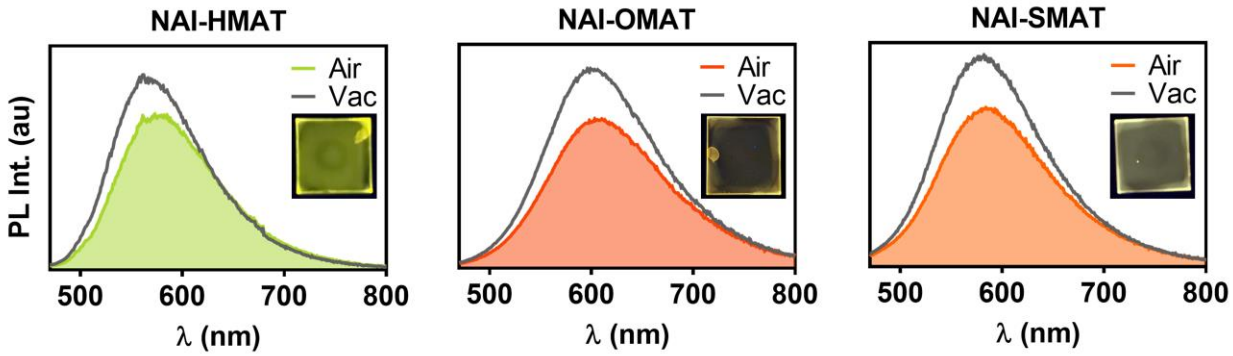

Figure S14. Emission spectra of 3 wt% doped PMMA films measured in vacuum and air, with inset photos of films irradiated under 365 nm light.

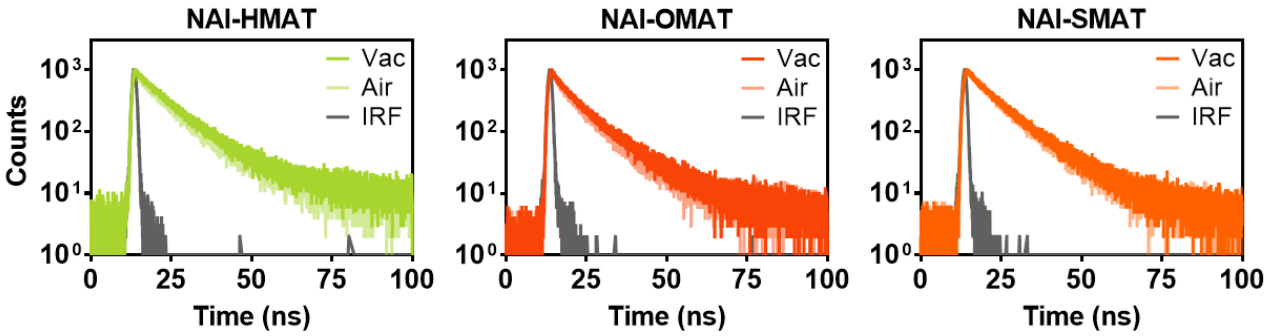

Figure S15. Prompt photoluminescence decays of 3 wt% doped PMMA films in vacuum and aerated conditions (λ_{ex} = 380 nm).

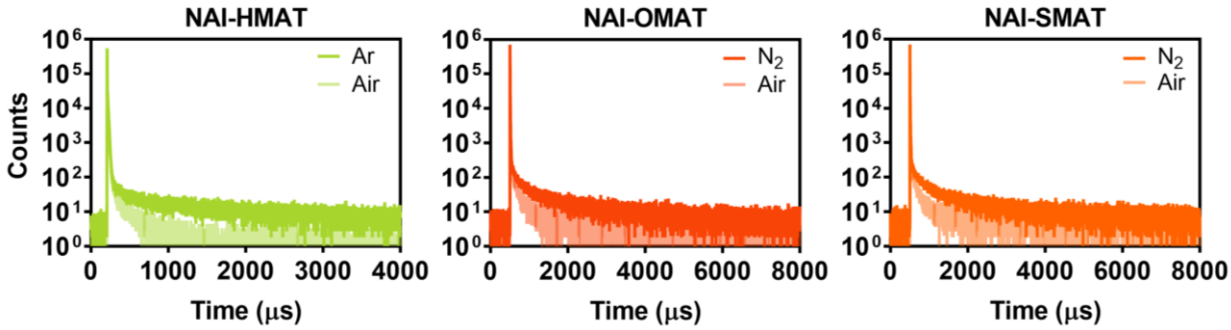

Figure S16. Time-resolved PL decay curves of 3 wt% PMMA doped films of all emitters under air and vacuum at 298 K.

Table S1. Emission properties of neat powder samples.

Entry	Pristine		Ground		Reversed	
	λ_{em} (nm)[a]	τ_{air} (ns)[a,b]	λ_{em} (nm)[a]	τ_{air} (ns)[a,b]	λ_{em} (nm)[a]	τ_{air} (ns)[a,b]
NAI-HMAT	580	6.0	604	11.6	574	5.8
NAI-OMAT	575	6.6	650	10.3	594	7.6
NAI-SMAT	566	7.3	649	10.1	564	6.8

[a] Measured at 298 K under air. [b] Excited using pulsed LED excitation at 380 nm, monitored at the emission maximum.

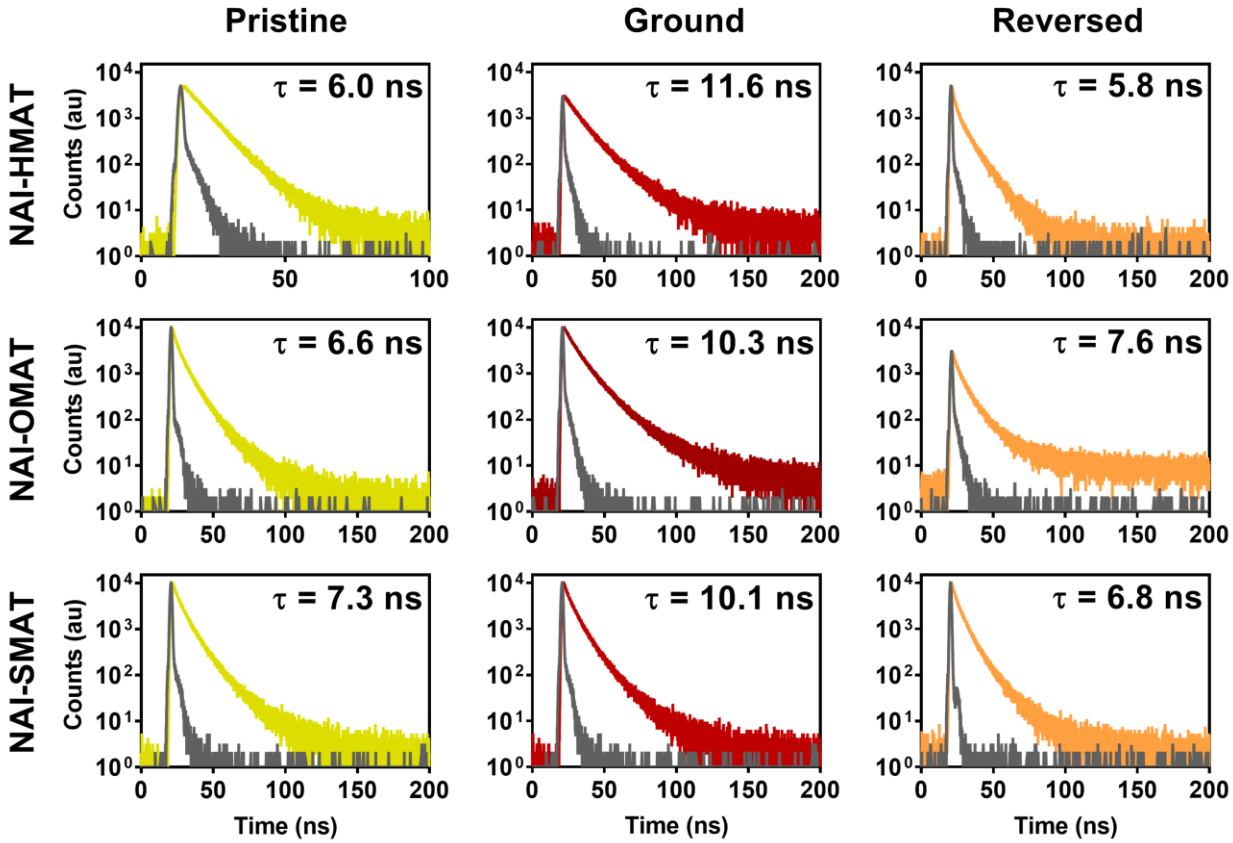

Figure S17. Time-resolved PL decay curves of 3 wt% PMMA doped films of all emitters under air and vacuum at 298 K.

X-ray Crystallography

Table S2. X-ray crystallographic data for **SMAT-TRZ**, **SOMAT-TRZ**, **SO_2MAT-TRZ**, **PTZO-TRZ**, and **$PTZO_2$-TRZ**.

	NAI-HMAT		NAI-HMAT
Formula	$C_{52.5}H_{48}N_2O_2$	***Z'***	1
$D_{calc.}$**/ g cm^{-3}**	1.301	**Wavelength/Å**	0.71073
/mm^{-1}	0.078	**Radiation type**	MoK
Formula Weight	738.93	Θ_{min}/°	1.488
Colour	orange	Θ_{max}/°	27.917
Shape	irregular-shaped	**Measured Refl's.**	53394
Size/mm^3	0.32×0.21×0.20	**Indep't Refl's**	8984
***T*/K**	100(2)	**Refl's I≥2 (I)**	7318
Crystal System	monoclinic	R_{int}	0.0323
Space Group	$P2_1/n$	**Parameters**	793
***a*/Å**	9.8194(12)	**Restraints**	2317
***b*/Å**	17.511(2)	**Largest Peak**	0.794
***c*/Å**	22.118(3)	**Deepest Hole**	-0.907
α/°	90	**GooF**	1.101
β/°	97.445(2)	wR_2 **(all data)**	0.1649
γ/°	90	wR_2	0.1568
V/Å^3	3771.2(8)	R_1 **(all data)**	0.0848
Z	4	R_1	0.0691

Crystal Data for NAI-HMAT. $C_{52.5}H_{48}N_2O_2$, M_r = 738.93, monoclinic, $P2_1/n$ (No. 14), a = 9.8194(12) Å, b = 17.511(2) Å, c = 22.118(3) Å, β = 97.445(2)°, $\alpha = \gamma$ = 90°, V = 3771.2(8) Å^3, T = 100(2) K, Z = 4, Z' = 1, μ(MoK$_\alpha$) = 0.078, 53394 reflections measured, 8984 unique (R_{int} = 0.0323) which were used in all calculations. The final wR_2 was 0.1649 (all data) and R_1 was 0.0691 (I≥2 σ(I)).

An orange irregular-shaped-shaped crystal with dimensions 0.32 × 0.21 × 0.20 mm^3 was mounted on a MITIGEN holder in oil. Data were collected using a Bruker APEX II area detector diffractometer operating at T = 100(2) K.

Data were measured using ϕ and ω scans of 0.5 ° per frame for 20 s using MoK$_\alpha$ radiation (microfocus sealed X-ray tube, 50 kV, 0.99 mA). The total number of runs and images was based on the strategy calculation from the program APEX4. The maximum resolution that was achieved was Θ = 27.917° (0.76 Å).

The unit cell was refined using SAINT V8.40B on 9848 reflections, 18% of the observed reflections. Data reduction, scaling and absorption corrections were performed using SAINT V8.40B. The final completeness is 99.60 % out to 27.917° in Θ.

SADABS-2016/2 was used for absorption correction.[5] wR_2(int) was 0.0463 before and 0.0432 after correction. The ratio of minimum to maximum transmission is 0.9512. The λ/2 correction factor is not present. The absorption coefficient μ of this material is 0.078 mm^{-1} at this wavelength (λ =

0.71073Å) and the minimum and maximum transmissions are 0.936 and 0.985.

The structure was solved and the space group $P2_1/n$ (# 14) determined by the XT structure solution program using Intrinsic Phasing methods and refined by full matrix least squares minimisation on F^2 using version 2018/3 of XL (Sheldrick, 2015).[6,7] The material crystallizes with disorder and refinements were carried out with restraints designed to maintain similar geometries between the two disordered fragments. The minor disordered fragment has an occupancy of ~11%. Finally, solvent toluene is found in the lattice, residing on an inversion center. A rigid group was used to model this solvent molecule. All non-hydrogen atoms were refined anisotropically. Hydrogen atom positions were calculated geometrically and refined using the riding model.

Powder X-ray diffraction patterns of each pristine, ground, and reversed sample were collected on a Malvern-Panalytical Empyrean 3 diffractometer using a Bragg-Brentano configuration. The compounds were not ground prior to collection of the diffraction pattern and were treated gently to not induce mechanical changes prior to measurement. The first powders were loosely packed into a steel sample holder with a 16 mm diameter well. Subsequent powders were gently packed into the shallow well of zero background Si substrates. Data was collected using Cu K_α radiation and scanned from $2\Theta = 5°–90°$. Due to the non-ideal nature of the sample, additional data were collected on each sample using (1) a parallel beam configuration to verify the peak positions and (2) using an area detector to inspect the diffraction rings and confirm their uniformity. Instrument details are provided in Table S3 below. In each case, the Bragg-Brentano scan was plotted in the manuscript.

Table S3. Instrument details for powder X-ray diffraction scans.

Instrument Type	Malvern-Panalytical Empyrean 3		
Configuration	Bragg-Brentano	Gonio scan with 2D detection	parallel beam
Tube	Cu LFF HR @ 45kV, 40mA		
Incident Beam Optics	iCore		
Divergence Slit	Fixed, 1/4°	Fixed, 1/2°	Fixed, 1/16°
Masks	14mm primary / 6mm secondary		
Soller Slits	0.03rad		
Filtration	Bragg-Brentano^{HD} (BBHD mirror)		
Sample Stage	Reflection/Transmission spinner – spinning on		
Accessory	Sample Changer		
Diffracted Beam Optics	dCore		
Soller Slits	0.04rad	none	none
Anti-scatter slit	Fixed, 1/4°	Fixed, 4°	open
Collimator	none	none	0.11° parallel plate
Detector	PIXcel^{3D} in 1D mode	PIXcel^{3D} in 2D mode	PIXcel^{3D} in 0D mode

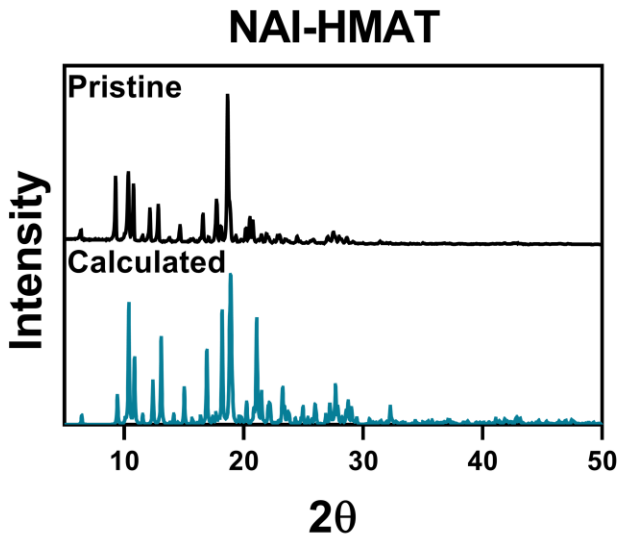

Figure S18. Experimental and calculated powder X-ray diffraction patterns for NAI-HMAT. The calculated pattern was generated from the single crystal data using the program Mercury (CCDC).

Thermal and Electrochemical Characterization

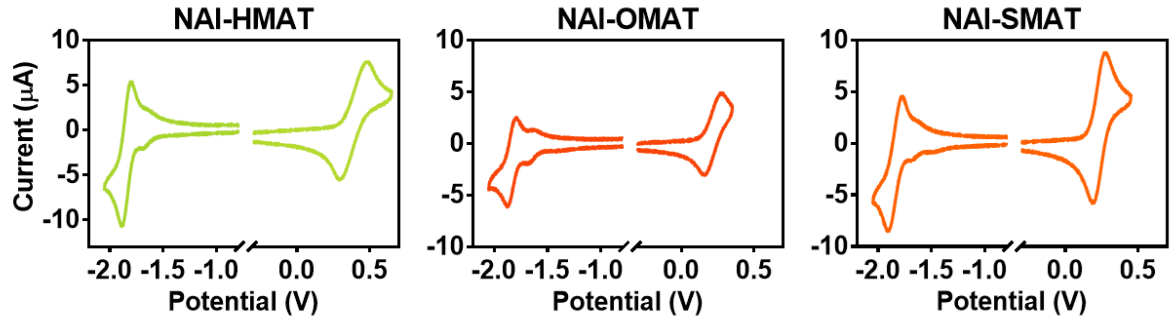

Figure S19. Cyclic voltammograms measured at 1 μmol mL^{-1} in degassed *o*-difluorobenzene relative to $Fc^{0/+}$, with 0.2 M [*n*-Bu_4N^+][PF_6^-] at 50 mV s^{-1}. Each sample was run with three cycles, with the third cycle shown in each case.

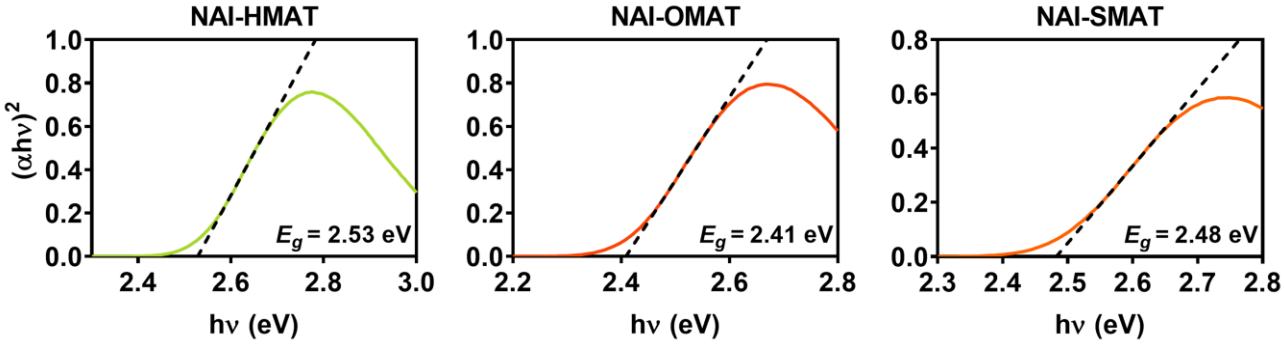

Figure S20. Tauc plots determined using absorption spectra measured in toluene, with calculated optical gaps (E_g) displayed inset.

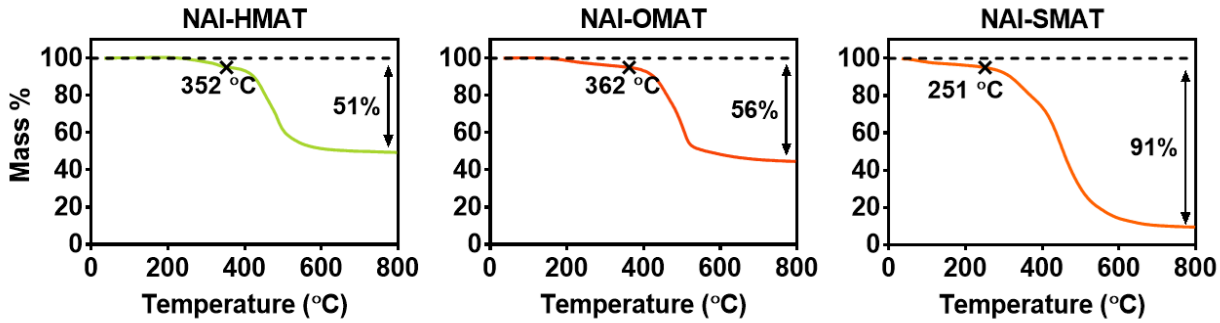

Figure S21. Thermogravimetric analysis (TGA) performed at a rate of 10 °C min^{-1}, under a 50 mL min^{-1} flow of nitrogen gas, from 30 to 800 °C.

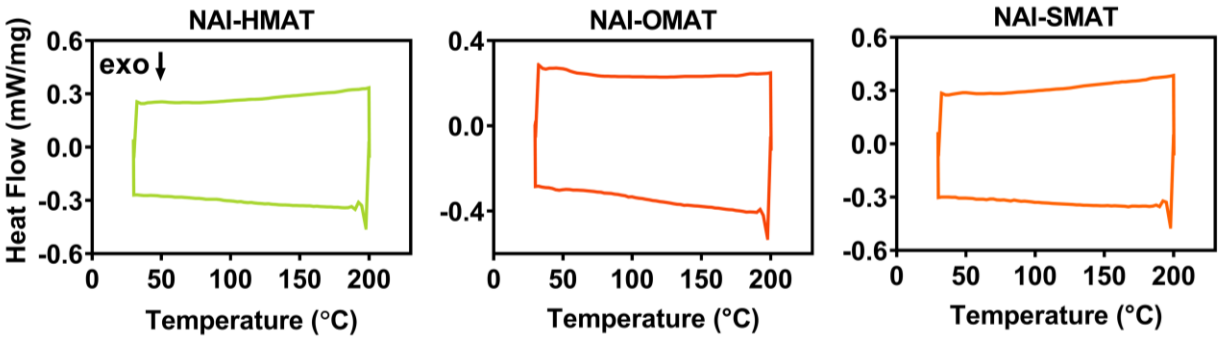

Figure S22. Differential scanning calorimetry (DSC) traces acquired at a rate of 10 °C min^{-1}, under a 50 mL min^{-1} flow of nitrogen gas. Two consecutive heating and cooling cycles were performed, with the first heating cycle shown in (A) and the second heating and cooling cycle shown in (B).

Density Functional Theory

Table S4. Results of DFT and TDA-DFT calculations.

Entry	HOMO[a] (eV)	LUMO[a] (eV)	E_{gap} (eV)	E_{S1}[b] (eV)	f[b] ($S_0 \rightarrow S_1$)	# Imag. Freq.	E_{Total} (10^3 Hartrees)
NAI-HMAT	–5.17	–2.69	2.49	2.13	0.2288	0	–2.154
NAI-OMAT	–5.04	–2.70	2.34	1.99	0.2258	0	–2.111
NAI-SMAT	–5.24	–2.72	2.52	2.17	0.2075	0	–2.434

[a] Calculated at the B3LYP/6-31+g(d) level. [b] Calculated using TDA-DFT at the B3LYP/6-31+g(d) level in toluene using a polarized continuum model.

Table S5. Cartesian coordinates [Å] of the optimized structure for **NAI-HMAT.**

	X	Y	Z		X	Y	Z		X	Y	Z
C	3.025026	-2.02936	-2.14014	C	-5.454361	2.504036	-0.251681	H	-9.021609	-2.617023	0.413621
C	1.629957	-2.10362	-2.31797	C	-3.949629	2.710296	-0.249275	H	-9.310955	2.275444	-0.320117
C	0.784103	-1.30991	-1.56735	C	-7.337208	-1.299597	0.265304	H	-8.225916	4.476371	-0.616210
C	1.292336	-0.40606	-0.59577	C	-8.265677	-0.115638	0.060134	H	-5.757682	4.601810	-0.572057
C	2.713235	-0.30341	-0.45252	C	-7.483590	1.175142	-0.107400	H	-3.571366	-2.249335	2.731641
C	3.561256	-1.13709	-1.22809	C	-5.817142	-3.593424	0.663559	H	-3.581452	-3.915479	2.126793
C	0.450319	0.431392	0.211135	C	-7.199020	-3.704549	0.636935	H	-2.107387	-2.946447	2.013938
C	1.041551	1.358449	1.062082	C	-7.939576	-2.549603	0.436850	H	-2.018891	-3.384153	-0.540687
C	2.437102	1.46744	1.180925	C	-8.228811	2.342284	-0.300434	H	-3.494173	-4.347407	-0.435936
C	3.270028	0.639268	0.448485	C	-7.629394	3.581212	-0.467910	H	-3.419989	-2.969866	-1.548052
C	4.735819	0.757303	0.61291	C	-6.244355	3.641592	-0.441118	H	-3.870237	3.281033	1.862171
N	5.526899	-0.11275	-0.16312	C	-3.198468	-2.907805	1.940393	H	-2.494807	3.878259	0.914794
C	5.035011	-1.05804	-1.08225	C	-3.111699	-3.330433	-0.561088	H	-4.072540	4.657772	0.764262
C	9.068936	0.935575	-0.66847	C	-3.573006	3.693125	0.892309	H	-4.017201	4.263522	-1.803604
C	7.688154	0.850034	-0.81966	C	-3.518855	3.307933	-1.616332	H	-2.439403	3.483320	-1.649526
C	6.960013	-0.01894	-0.01123	C	11.853972	-0.626236	1.506414	H	-3.779112	2.622524	-2.429534
C	7.609006	-0.79488	0.939819	C	11.940261	-0.085218	-0.929958	H	12.941021	-0.496901	1.558413
C	8.995186	-0.70152	1.083616	C	11.640367	1.751195	0.772827	H	11.444591	-0.389045	2.495143
C	9.754857	0.163419	0.28503	C	-9.197594	0.014965	1.295567	H	11.656008	-1.683384	1.295025
O	5.802781	-1.76711	-1.71735	C	-9.119238	-0.357741	-1.214401	H	13.031340	0.000299	-0.853462
O	5.25802	1.558363	1.375578	H	3.699853	-2.650915	-2.719346	H	11.609081	0.568995	-1.743103
C	11.27894	0.292181	0.414619	H	1.218237	-2.783570	-3.058048	H	11.694774	-1.116365	-1.208506
C	-1.02477	0.327095	0.165571	H	-0.286300	-1.361240	-1.730312	H	11.178580	2.044591	1.722454
C	-1.68786	-0.88655	0.339213	H	0.404732	1.986475	1.678154	H	12.727683	1.859759	0.870678
C	-3.07733	-0.99669	0.332758	H	2.883082	2.184786	1.862117	H	11.301271	2.453830	0.004586
C	-3.8751	0.15615	0.139106	H	9.618446	1.619234	-1.308570	H	-8.606195	0.185730	2.201028
C	-3.218	1.397759	-0.0307	H	7.173189	1.453604	-1.561180	H	-9.893145	0.851325	1.179580
C	-1.82438	1.454476	-0.00813	H	7.034185	-1.470233	1.566632	H	-9.790472	-0.892756	1.441460
C	-3.64921	-2.38665	0.548895	H	9.476069	-1.318494	1.833614	H	-9.813230	0.469899	-1.388359
C	-5.16676	-2.36772	0.494346	H	-1.095115	-1.776984	0.513101	H	-8.472275	-0.451185	-2.092762
C	-5.92768	-1.19305	0.291072	H	-1.336113	2.411488	-0.154215	H	-9.709672	-1.274550	-1.126415
N	-5.28913	0.069028	0.117604	H	-5.221146	-4.485527	0.821688				
C	-6.07183	1.243544	-0.07928	H	-7.685974	-4.666018	0.769554				

Table S6. Cartesian coordinates [Å] of the optimized structure for **NAI-OMAT.**

	X	Y	Z		X	Y	Z		X	Y	Z
C	2.610338	-2.024779	-2.147654	C	-6.314753	-1.195490	0.293711	H	-1.499178	-1.792777	0.509953
C	1.215506	-2.100754	-2.326492	N	-5.668299	0.050816	0.122548	H	-1.750666	2.404683	-0.150144
C	0.367937	-1.311191	-1.573410	C	-6.462424	1.205481	-0.069025	H	-5.765873	-4.506610	0.816919
C	0.873898	-0.409995	-0.598197	C	-5.901986	2.477660	-0.243560	H	-8.231728	-4.564066	0.754779
C	2.294631	-0.304987	-0.454435	C	-4.395395	2.701311	-0.244153	H	-9.497573	-2.415257	0.391255
C	3.144473	-1.134589	-1.232380	C	-7.721109	-1.251153	0.263436	H	-9.769630	2.010504	-0.273007
C	0.029979	0.423147	0.211515	O	-8.493399	-0.130520	0.071858	H	-8.776397	4.305795	-0.584673
C	0.619750	1.349130	1.064864	C	-7.864488	1.081211	-0.087501	H	-6.322772	4.563111	-0.562600
C	2.015008	1.460844	1.183741	C	-6.315523	-3.585097	0.658917	H	-4.001815	-2.289700	2.732033
C	2.849605	0.636242	0.449177	C	-7.703369	-3.624564	0.625789	H	-4.033775	-3.952021	2.115410
C	4.315161	0.756847	0.614025	C	-8.413310	-2.440867	0.425189	H	-2.547208	-3.000104	2.007436
N	5.108084	-0.109431	-0.164283	C	-8.696958	2.174188	-0.269389	H	-2.464866	-3.429534	-0.540575
C	4.618136	-1.053276	-1.085834	C	-8.137259	3.440106	-0.441306	H	-3.952847	-4.375449	-0.434688
C	8.648069	0.946672	-0.667732	C	-6.755354	3.577818	-0.427340	H	-3.860712	-3.000217	-1.549609
C	7.267471	0.858642	-0.819153	C	-3.638003	-2.947688	1.936273	H	-4.319955	3.275770	1.866875
C	6.541037	-0.013042	-0.012115	C	-3.557155	-3.363468	-0.562256	H	-2.957733	3.892922	0.912452
C	7.191473	-0.789185	0.937776	C	-4.033012	3.690140	0.894974	H	-4.549887	4.645653	0.764611
C	8.577449	-0.693277	1.081819	C	-3.979760	3.308868	-1.609977	H	-2.903250	3.502262	-1.643988
C	9.335457	0.174404	0.284622	C	11.436023	-0.612993	1.504939	H	-4.230444	2.622945	-2.425641
O	5.387139	-1.759436	-1.722602	C	11.521448	-0.067861	-0.930568	H	-4.495279	4.257016	-1.790236
O	4.835449	1.556990	1.378928	C	11.217677	1.765201	0.775159	H	12.522792	-0.481523	1.557288
C	10.859266	0.306028	0.414568	H	3.286556	-2.643099	-2.728690	H	11.026052	-0.378248	2.494008
C	-1.445218	0.315663	0.166345	H	0.805362	-2.778484	-3.069478	H	11.240262	-1.670201	1.291800
C	-2.099766	-0.906387	0.339331	H	-0.702225	-1.363611	-1.737712	H	12.612334	0.019733	-0.853820
C	-3.487987	-1.022958	0.334641	H	-0.018032	1.973722	1.683447	H	11.189044	0.587010	-1.742682
C	-4.270659	0.140022	0.142561	H	2.459530	2.177126	1.867000	H	11.278079	-1.099049	-1.210812
C	-3.635610	1.392553	-0.027704	H	9.196279	1.632383	-1.306748	H	10.755177	2.056158	1.725189
C	-2.242675	1.448785	-0.005787	H	6.751365	1.462312	-1.559801	H	12.304751	1.875789	0.873344
C	-4.081685	-2.415326	0.548193	H	6.617957	-1.466637	1.563524	H	10.877302	2.468380	0.007982
C	-5.603416	-2.385735	0.495299	H	9.059505	-1.310442	1.830903				

Table S7. Cartesian coordinates [Å] of the optimized structure for **NAI-SMAT.**

	X	Y	Z		X	Y	Z		X	Y	Z
C	2.747432	-2.059274	-2.095281	C	-6.115410	-1.236978	0.199925	H	-1.314974	-1.741900	0.685099
C	1.348956	-2.140052	-2.241053	N	-5.493516	0.027295	-0.046499	H	-1.579083	2.438794	-0.017783
C	0.517591	-1.331121	-1.490638	C	-6.273792	1.216181	-0.199112	H	-5.521097	-4.307485	1.544372
C	1.044763	-0.404276	-0.551227	C	-5.709704	2.495892	-0.036328	H	-7.953685	-4.558771	1.206364
C	2.468221	-0.297728	-0.439267	C	-4.210306	2.728892	0.043568	H	-9.198224	-2.720277	0.040395
C	3.301220	-1.146704	-1.214451	C	-7.477173	-1.458098	-0.111818	H	-9.514642	2.174856	-0.752968
C	0.218881	0.450291	0.254327	S	-8.368790	-0.336346	-1.141453	H	-8.532668	4.428328	-0.256752
C	0.826674	1.391586	1.077404	C	-7.646155	1.155044	-0.535523	H	-6.094362	4.603510	0.086113
C	2.224267	1.502968	1.166304	C	-6.083547	-3.490761	1.105401	H	-3.871666	-1.794092	3.002211
C	3.042481	0.662432	0.431707	C	-7.446991	-3.647310	0.904351	H	-3.870792	-3.542675	2.705565
C	4.511569	0.784756	0.563735	C	-8.141068	-2.622702	0.268603	H	-2.391233	-2.605603	2.459794
N	5.287568	-0.096048	-0.214794	C	-8.458173	2.287445	-0.528528	H	-3.600979	-3.274560	-1.071550
C	4.777707	-1.063215	-1.100941	C	-7.910093	3.538930	-0.265558	H	-2.234892	-3.508382	0.037563
C	8.822934	0.935835	-0.820945	C	-6.541618	3.625942	-0.056548	H	-3.724808	-4.425738	0.269736
C	7.434353	0.844063	-0.940009	C	-3.480043	-2.583463	2.352494	H	-2.788520	3.703518	1.401730
C	6.723508	0.002397	-0.094946	C	-3.325706	-3.451573	-0.026697	H	-4.377871	4.475996	1.368014
C	7.392048	-0.748130	0.868662	C	-3.863871	3.510524	1.338550	H	-4.161351	2.936799	2.222279
C	8.775823	-0.649224	0.979255	C	-3.783847	3.559041	-1.196912	H	-4.016307	3.014880	-2.117934
C	9.523617	0.193482	0.138760	C	11.656457	-1.133515	0.072822	H	-4.309547	4.517787	-1.225394
O	5.532740	-1.786345	-1.735172	C	11.695413	1.239238	-0.704592	H	-2.710342	3.769638	-1.184404
O	5.047507	1.598733	1.302708	C	11.389678	0.752943	1.725727	H	12.747456	-1.096103	0.181924
C	11.048403	0.268985	0.298483	H	3.410910	-2.692406	-2.675051	H	11.272579	-1.863311	0.793180
C	-1.257110	0.344710	0.236169	H	0.922916	-2.837651	-2.956142	H	11.423826	-1.501310	-0.933022
C	-1.912935	-0.866887	0.457484	H	-0.556034	-1.389608	-1.628082	H	12.780193	1.256422	-0.549548
C	-3.301667	-0.982919	0.452582	H	0.203048	2.030345	1.695879	H	11.326386	2.263366	-0.576454
C	-4.094700	0.151006	0.157645	H	2.683497	2.232356	1.825523	H	11.513896	0.933750	-1.741488
C	-3.455162	1.408742	0.068486	H	9.352862	1.600141	-1.493448	H	10.998503	0.072821	2.489470
C	-2.061470	1.473543	0.089018	H	6.905868	1.425929	-1.689355	H	12.477308	0.813958	1.855813
C	-3.886101	-2.321359	0.877971	H	6.828839	-1.403923	1.526007	H	10.964796	1.745866	1.911997
C	-5.399987	-2.317746	0.750130	H	9.278308	-1.242566	1.737219				

References

1 A. H. Balawi, S. Stappert, J. Gorenflot, C. Li, K. Müllen, D. Andrienko and F. Laquai, *J. Phys. Chem. C*, 2019, **123**, 16602–16613.

2 Z. Fang, T. L. Teo, L. Cai, Y. H. Lal, A. Samoc and M. Samoc, *Org. Lett.*, 2009, **11**, 1–4.

3 S. Kataoka, S. Suzuki, Y. Shiota, K. Yoshizawa, T. Matsumoto, M. S. Asano, T. Yoshihara, C. Kitamura and S. I. Kato, *J. Org. Chem.*, 2021, **86**, 12559–12568.

4 J. Zhou, P. Chen, X. Wang, Y. Wang, Y. Wang, F. Li, M. Yang, Y. Huang, J. Yu and Z. Lu, *Chem. Commun.*, 2014, **50**, 7586–7589.

5 L. Krause, R. Herbst-Irmer, G. M. Sheldrick and D. Stalke, *J. Appl. Crystallogr.*, 2015, **48**, 3–10.

6 G. M. Sheldrick, *Acta Crystallogr. Sect. A*, 2015, **A71**, 3–8.

7 G. M. Sheldrick, *Acta Crystallogr. Sect. C*, 2015, **C71**, 3–8.